Nanostructures and Dynamics of Macromolecules Bound to Attractive Filler Surfaces

Naisheng Jiang,[†] Maya K. Endoh,[†,‡] Tadanori Koga,*[,†,‡,§] Tomomi Masui,[‖] Hiroyuki Kishimoto,[‖] Michihiro Nagao,[⊥,#] Sushil K. Satija,[⊥] and Takashi Taniguchi[○]

[†]Department of Materials Science and Engineering, [‡]Department of Chemistry, and [§]Chemical and Molecular Engineering Program, Stony Brook University, Stony Brook, New York 11794, United States

[‖]Sumitomo Rubber Industries Ltd., 1-1, 2-chome, Tsutsui-cho, Chuo-ku, Kobe, 671-0027, Japan

[⊥]NIST Center for Neutron Research, National Institute of Standards and Technology, Gaithersburg, Maryland 20899-6102, United States

[#]Center for Exploration of Energy and Matter, Indiana University, Bloomington, Indiana 47408, United States

[○]Graduate School of Engineering, Department of Chemical Engineering, Kyoto University, Katsura-Campus, Nishikyo-ku, Kyoto, 615-8510, Japan

S *Supporting Information*

ABSTRACT: We report in situ nanostructures and dynamics of polybutadiene (PB) chains bound to carbon black (CB) fillers (the so-called "bound polymer layer (BPL)") in a good solvent. The BPL on the CB fillers was extracted by solvent leaching of a CB-filled PB compound and subsequently dispersed in deuterated toluene to label the BPL for small-angle neutron scattering and neutron spin echo techniques. The results demonstrate that the BPL is composed of two regions regardless of molecular weights of PB: the inner unswollen region of ≈ 0.5 nm thick and outer swollen region where the polymer chains display a parabolic profile with a diffuse tail. In addition, the results show that the dynamics of the swollen bound chains can be explained by the so-called "breathing mode" and is generalized with the thickness of the swollen BPL.
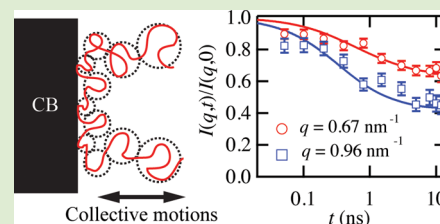
Polymer nanocomposites have been of great interest to the broad materials community for at least the last three decades.[1] The addition of nanoparticles to polymers affects the overall rheological and mechanical properties mainly due to the creation of a "bound polymer layer (BPL)" on a particle surface.[2−10] The most thorough experimental and theoretical studies on BPLs have been carried out on carbon black (CB)-filled rubber systems[11−16] used for automobile tires. A nanometer-thick BPL is typically formed on the CB surfaces and is resistant to dissolution even in a good solvent.[17] In theory, the interactions between polymers and particle surfaces restrict a molecular motion which correlates with increased resistance to mechanical deformation as compared to free polymers that locate away from the particle surface.[18] This restricted chain motion was indicative in various polymer nanocomposites by nuclear magnetic resonance (NMR) spectroscopy experiments.[5−8,19,20] In addition, the existence of an "interphase" with the property between those of the BPL and the bulk has been hypothesized as the origin of long-range propagations of the effects of the BPL.[21−25] However, it is challenging to distinguish the bound polymer chains or the interphase from the bulk experimentally, because they are all composed of the same component.[25,26] Hence, a molecular scale description of real conformations of the bound polymer chains, which is crucial for a better understanding of the reinforcement mechanism at the interface, remains unclear.[7,27]

To overcome this difficulty and provide detailed nanometer-scale descriptions at the polymer/filler interface, we use small-angle neutron scattering (SANS) and neutron spin echo (NSE). In addition, we use simplified industrial polybutadiene (PB)/CB nanocomposites as a model. A novel aspect of CB along with its practical importance is the scattering length density that is nearly identical to those of deuterated solvents or polymers, allowing "contrast matching" neutron scattering experiments[28] to gain information about the bound polymer chains selectively. Furthermore, as will be discussed later, the PB bound layer on the CB filler can be considered as a "slab" configuration such that neutron reflectivity (NR) can also be used as a complementary tool to investigate the polymer concentration profile (in the direction normal to the solid surface) in a solvent. We here focus on the CB fillers with the BPL dispersed in a good solvent where the unique collective dynamics of the bound chains is revealed within the time and space domains of the NSE technique. The experimental findings would be then useful to discuss how the structures and dynamics are altered when the bound polymer chains entangle with free polymer chains in polymer solutions.
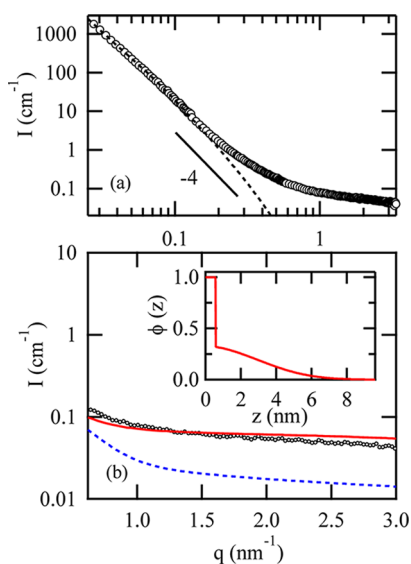
A spherical CB filler (the density of 1.8 g/cm^3) with mostly nonfused aggregates (Asahi Carbon Co., Japan) was used.[29] The mean radius (R_{TEM}) of the CB filler was determined to be (43 ± 20) nm from transmission electron microscopy (TEM) experiments (Supporting Information). Three different kinds of hydrogenated polybutadiene (hPB) were utilized for the SANS/NSE experiments: Two are monodisperse hPB (number-average molecular weight (M_n) = 38 kg/mol, polydispersity (M_w/M_n) = 1.05, Polymer Source, Inc.), and M_n = 115 kg/mol (M_w/M_n = 1.03, Sumitomo Rubber) as models; the other is relatively polydisperse hPB (M_n = 157 kg/mol, M_w/M_n = 2.7, Ube Industries, ltd. Japan) to discuss the polydispersity effect on the structure of the BPL (Supporting Information). Hereafter we denote them as PB38k, PB115k, and PB157k, respectively. The preparation of the hPB bound layer on the CB filler is summarized in Supporting Information. The thicknesses of the BPL were estimated to be (4.5 ± 0.5) nm for PB38k and (7.0 ± 0.5) nm for PB115 K and PB157k, respectively. Hereafter we assign the CB filler covered with the BPL layer as "BPL-coated CB". To label the BPL for the SANS and NSE experiments, deuterated toluene (d-toluene, degree of deuteration of 99.8 %, Cambridge Isotope Laboratories, Inc., MA) was used: the scattering length density (SLD$_{d\text{-toluene}}$ = 5.7 × 10^{-4} nm^{-2}) is nearly identical to that of the CB filler (SLD$_{CB}$ = 6.0 × 10^{-4} nm^{-2}). The BPL-coated CB fillers were dispersed in d-toluene using an ultrasonic bath. The volume fraction of the CB fillers (ϕ) was fixed to 1.8 % so as to prevent aggregation of the CB fillers. We confirmed that the BPL-coated CB fillers were stable in d-toluene for at least 30 days (i.e., no precipitation).

Figure 1a shows a representative SANS profile from the BPL(PB38k)-coated CB in d-toluene at 25 °C. SANS profiles

were measured as a function of the scattering vector, $q = (4\pi \sin \theta)/\lambda$, where 2θ is the scattering angle and λ is the neutron wavelength. Since distinct scattering maxima from a core−shell type form factor are not clearly seen, we utilized the unified equation for hierarchical structural analysis of nanoparticles[30] with further consideration of an interfacial root-mean-square roughness (σ) between the BPL-coated CB and d-toluene:[31]

$$I(q) = A \, \exp\left(-\frac{q^2 R_{g,BR}^2}{3}\right) q^{-\alpha} + B \, \exp\left(-\frac{q^2 R_{g,BR}^2}{3}\right)$$
$$+ C\left[\mathrm{erf}\left(\frac{q R_{g,BR}}{\sqrt{6}}\right)^3 / q\right]^{\beta} \exp(-\sigma^2 q^2) \tag{1}$$

where $R_{g,BR}$ is the radius of gyration of the entire BPL-coated CB fillers, and α, β, A, B, and C are numerical constants. The σ value of 2.3 nm was used based on a NR experimental result about a BPL mimicked on a chemically similar flat surface, as shall be discussed later. The detail of the fitting using eq 1 is summarized in Supporting Information. The best-fit to the data (the dotted line in Figure 1a) in the low-q region ($q < 0.1$ nm^{-1}) gave us the $R_{g,BR}$ value of (57 ± 1) nm. At the same time, the bare CB fillers (without the BPL) dispersed into d-toluene were characterized using small-angle X-ray scattering at the beamline x27C, National Synchrotron Light Source (Upton, NY). The same analysis using eq 1 (excluding the contribution of σ) gave the radius of gyration ($R_{g,CB}$) of the pure CB fillers to be (49 ± 1) nm, which is 1.5 × larger than that of the primary CB particles ($R_{g,TEM} = (3/5)^{1/2} R_{TEM} = 33$ nm). Based on the volume consideration, it is reasonable to deduce that about 3 (= $(R_{g,CB}/R_{g,TEM})^3$) CB primary particles are fused together into the aggregates.[32,33] The total thickness of the swollen BPL (l) is then approximated $l = R_{g,BR} − R_{g,CB} = 8$ nm for PB38k. Hence, the BPL swells in the solvent, as previously reported.[31] Note that no significant temperature dependence of the structure was observed.

Another important feature of the SANS profile is the excess scattering at high q, that is, the deviation from eq 1 (Figure 1a). Figure 1b shows the excess scattering (black symbols) after subtraction of the scattering intensity computed by eq 1 from the observed SANS data.[34] It should be emphasized that the polydispersity effect of the filler size is not crucial for the estimation of the excess scattering at $q > 0.2$ nm^{-1}. As will be discussed below, the observed SANS data consists of two contributions: the static structure factor $S(q)$ of the BPL and density fluctuations in the BPL. To evaluate the two contributions separately, the following strategies were combined: The CB filler is approximated as a "planar" geometry since the size of the CB aggregates by far exceeds the BPL thickness; we thus mimic a BPL on a chemically similar flat substrate such that the polymer concentration profile in the direction normal to the solid, $\phi(z)$, can be independently studied by using NR. $S(q)$ can be then calculated by

$$S(q) = \left|\int_0^L \rho_0 \phi(z) \exp(iqz) dz\right|^2 \tag{2}$$

where ρ_0 is a contrast difference between the polymer and solvent. For this purpose, we deposited a carbon layer via sputtering on a Si substrate (Supporting Information). To prepare the BPL on the substrate, we reproduced the established protocol for PB:[35] An approximately 80 nm thick deuterated PB (dPB, M_w = 233 kg/mol, M_w/M_n = 1.14,

Figure 1. (a) SANS profile of the BPL (PB38k)-coated CB in d-toluene at 25 °C. Note the incoherent scattering intensity is subtracted from the data. (b) Excess scattering (symbols) after subtraction of the filler scattering calculated by eq 1 (dotted line in (a)). The red solid line corresponds to the best-fit to the data based on the volume fraction profile of the BPL vs the distance (z) from the CB surface shown in the inset. The dashed blue line corresponds to $S(q)$ in eq 5 and the difference between the red and blue lines corresponds to the contribution from the fluctuations, that is, the origin of the breathing dynamics.

Polymer Source) spin-cast film on the carbon-coated Si substrate was annealed at 100 °C for up to 72 h under vacuum; the film was then leached in baths of continuously replenished toluene at 20 °C until the thickness of the residue layer remained unchanged. We confirmed that the homogeneous dPB bound layer of (4.9 ± 0.5) nm in thickness (in the dry state) was formed on the substrate (Supporting Information). Further in situ NR results evidenced that $\phi(z)$ of the dPB bound layer in hydrogenated toluene (h-toluene, Sigma-Aldrich, ACS reagent, >99.5 %) can be well approximated as a parabolic function with the inclusion of a tail (Supporting Information), as experimentally reported for an end-grafted polymer chain in a good solvent.[36] Hence, to a first approximation, the $\phi(z)$ data can be used to represent the swollen BPL on the CB filler. Below we demonstrate how to refine $\phi(z)$ from the simultaneous fits of the SANS and NSE data.

Figure 2 shows representative normalized intermediate dynamic structure factors (i.e., $I(q,t)/I(q,0)$) of the BPL-coated
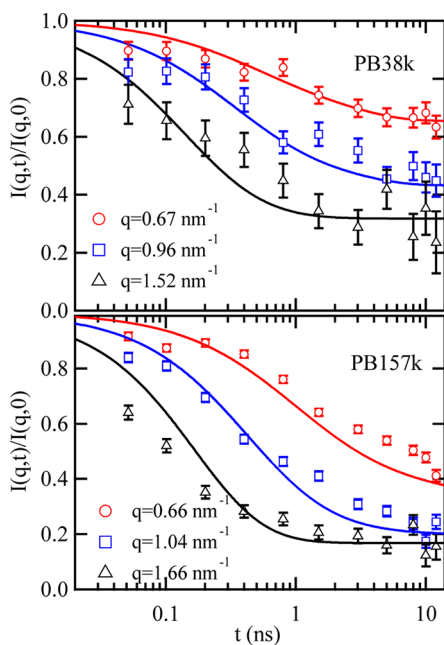
Figure 2. Measured $I(q,t)/I(q,0)$ (symbols) and best-fits of the breathing model (lines) at the three different q values at 50 °C. The error bars represent ± 1 standard deviation.

CB with the two different hPB in d-toluene at 50 °C. From the figure we can see that even at the largest q value used ($q = 1.66$ nm^{-1}), all the $I(q,t)/I(q,0)$ functions are not fully relaxed at the Fourier times of up to 20 ns. However, the q-dependence of the plateau-like behavior indicates that the polymer chains are still in motion in the solvent.[25] Hence, the overall dynamic structure factors including the tails cannot be described by segmental chain dynamics in a solvent, such as the Rouse model[37] and Zimm model.[38] We instead assume that the initial fast decay and slow tail is attributed to collective motions[39−41] of the bound polymer chains. On the theoretical side, de Gennes elucidated the collective relaxation process of physically adsorbed polymer chains in a good solvent: the so-called breathing mode determined by a balance of a restoring force due to the osmotic pressure gradient and a viscous force exerted on a polymer.[42] Farago and co-workers[39] formulated

the dynamic structure factors of tethered chains in a solvent accounted for the breathing mode.

To quantify the NSE data based on the breathing mode, we continuously approximate the planar geometry such that the equation of a local displacement $u(z,t)$ of the adsorbed chains along the normal (z) direction of the surface is given by[39]

$$\frac{\partial}{\partial z}\left(E(z)\frac{\partial u}{\partial z}\right) = \frac{6\pi \eta_s}{\xi^2}\frac{\partial u}{\partial t} \quad (3)$$

where $E(z)$, η_s, and ξ are the osmotic compressibility, the viscosity of the solvent, and the correlation length (i.e., a blob size),[43] respectively. On the basis of the scaling theory for semidilute solutions,[43] the relations of $\xi = cz$ and $E(z) = E_0 k_B T/\xi^3$ (c and E_0 are numerical constants, and k_B is the Boltzmann constant) are given. As for the time decay, eq 3 has a solution of a simple exponential function:[39]

$$u(z, t) = u_n(z)\exp(-t/\tau_n) \quad (4)$$

In addition, due to the boundary conditions, eq 3 is a Sturm−Liouville boundary value problem with eigenvalues, $1/\tau_n = (k_B T/6\pi \eta_s c)(E_0 \Lambda_n/(z_{max})^3)$, $\Lambda_n \simeq an^b + e$ ($n = 1, 2, ...$ and a, b, and e are constants) and eigen functions $u_n(z)$ for the displacement (Supporting Information). z_{max} corresponds to the maximum height of the BPL, including the tail. The intermediate dynamic structure factor with a mode n, $I_n(q,t)$, depends on the density fluctuation, $\delta \rho = d(\phi(z)u_n(z,t))/dz$, and $I(q,t)/I(q,0)$, which is given by the summation of contributions $I_n(q,t)$ from mode n ($n \leq 10$ in the present case), is given by the same protocol established previously:[39]

$$\frac{I(q, t)}{I(q, 0)} = \frac{S(q) + \sum_n^\infty \frac{2}{E_0 \Lambda_n}\tilde{q}^2 |(\phi|\zeta_n)|^2 \exp(-\gamma E_0 \Lambda_n t)}{S(q) + \sum_n^\infty \frac{2}{E_0 \Lambda_n}\tilde{q}^2 |(\phi|\zeta_n)|^2} \quad (5)$$

where $\gamma = (k_B T/6\pi \eta_s c)(1/(z_{max})^3)$. $(\phi|\zeta_n)$ represents

$$(\phi|\zeta_n) = \int_0^1 \phi(\tilde{z})\zeta_n(\tilde{z})e^{i\tilde{q}\tilde{z}}d\tilde{z} \quad (6)$$

with $\tilde{q} = qz_{max}$ and $\tilde{z} = z/z_{max}$. To optimize the two unknown parameters (E_0, γ) and $\phi(z)$, we simultaneously fit the NSE and SANS data (i.e., $I(q,0)$ in this case) for PB38k with eq 5 and the denominator of the right-hand side of eq 5 using a nonlinear least-squares data fitting. We found that, as shown in Supporting Information, both the SANS and NSE data could not be reasonably fit with $S(q)$ computed from the simple parabolic function $\phi(z)$. Instead, taking previous experimental[23,44,45] and computational[46] results into account, a two-layer structural model with inclusion of a less swollen adsorbed layer next to the filler surface was adopted:

$$\phi(z; z_1, L) = \begin{cases} \phi_a, & 0 \leq z < z_1 \\ \phi_m[1 - (z/L)^2], & z_1 \leq z < L \\ 0, & L \leq z \end{cases} \quad (7)$$

where ϕ_a is the polymer segment volume fraction of the adsorbed layer, ϕ_m is the extrapolated volume fraction to $z = 0$ from the pseudobrush part, and L is the cutoff thickness of the swollen pseudobrush layer. In addition, we introduced a tail to fit the data by convoluting eq 7 with a normalized Gaussian function.[36] As a result, it was found that the two-layer model (shown in the inset of Figure 1b) fits the SANS and NSE data

reasonably (the solid lines in Figure 1b and Figure 2). The best-fits indicate that the inner region of $z_1 = 0.5$ nm does not contain any solvent ($\phi_a = 1$), while the polymer chains in the outer region are expanded parabolically with $z_{max} = (8.0 \pm 1.0)$ nm and $\phi_m = (0.34 \pm 0.03)$ (the inset of Figure 1b). Note that we ignore the dynamics of the inner unswollen layer which would be too slow to see within the NSE time domain.[47] The same fitting protocol was applied to the SANS and NSE data for the BPL (PB157k)-coated CB in d-toluene. The best-fit results gave us a nearly identical $\phi(z)$ profile to that of the PB38k (the inner unswollen layer of ≈ 0.5 nm thick and $\phi_m = 0.34 \pm 0.03$), except $z_{max} = (11.0 \pm 1.0)$ nm for PB157k (data not shown). Hence, the following important conclusions are drawn: the conformations of the bound chains composed of the different chain lengths remain unchanged and $\phi(z)$ can be scaled with z_{max} of the swollen BPL layer. This is consistent with a self-consistent field study at the solid-polymer melt interface:[48] the fraction of loops per an adsorbed chain is nearly constant (≈ 30 %) for polymers at $N > 300$ (N: the degree of polymerization). At the same time, we found that the E_0 values, which relate to the chain elasticity and are predicted to be on the order of 1,[43] are nearly equivalent ($E_0 = 0.20 \pm 0.09$) for the two different PB. We will discuss this point later. It should be emphasized that the γ values obtained ($\gamma_{38K} = 0.11 \pm 0.06$ for PB38k and $\gamma_{157\ K} = 0.033 \pm 0.007$ for PB157k) hold the aforementioned relationship (i.e., $\gamma \propto 1/z_{max}^3$) with the same overall time scale of ≈ 1 ns. Hence, we may conclude that the breathing dynamics of the BPL can be generalized with the scaled thickness of the swollen BPL in the same (good) solvent when the size of the filler by far exceeds the BPL thickness.[49] Further experiments to explore various effects including the osmotic compressibility, grafting density, and the size of the nanofillers on the breathing mode[34] deserve future work.

Our SANS results remind us of previous NMR results which denoted two types of adsorbed chain segment sequences with different chain mobility in CB filled elastomers:[7,8] (i) chain fragments whose local mobility is significantly hindered at the filler surface, resulting in an immobilized polymer−filler interfacial layer of ≈ 0.6 nm thick; (ii) chain fragments located outside the immobilized interface whose large spatial scale mobility is constrained due to chain adsorption, i.e., the formation of loosely bound chains. It is known that irreversibly adsorbed polymer chains form three types of segment sequences, "trains", "loops", and "tails".[43] According to the molecular theory of rubber elasticity, stiffness of rubber depends on number density of "strands" between two neighboring entanglement points.[50] Provided that the loops of the bound polymer chains are regarded as the strands, it is reasonable to suppose that the bound chains with more loops become more elastic, as Patton and co-workers evidenced.[51] Hence, the aforementioned finding in E_0 suggests that the number density of the loops on the CB filler (i.e., the effective grafting density of the bound chains) is identical for the PB chains with different M_w. This may be supported by the experimental evidence that the degree of the chain expansion for the two different bound chains in the good solvent is comparable.[52]

In summary, with the rational design of the experimental system and a suite of experimental techniques, we could reveal the in situ structure and dynamics of the bound polymer chains on the filler surface at the nanometer scale. This detailed knowledge can then be used to fill the gap between the microscopic structure/dynamics and macroscopic properties.

Recently, Harton and co-workers[9] have demonstrated that the interfacial structure at the polymer−filler interface can be tuned by changing the curvature of the filler. Moreover, the density profile of a bound polymer chain to a nanoparticle surface may depend on the magnitude of a polymer-surface interaction.[46] Hence, systematic neutron scattering experiments with various types of polymers and nanoparticles would enable us to seek "nanoscale principles" at the interface.

ASSOCIATED CONTENT

$\mathbf{S}$ Supporting Information

Experimental procedures, a TEM image of the CB filler, NR results on the bare carbon layer coated Si substrate as well as the dPB bound layer on the carbon layer, the validity of the two-layer model used for the SANS and NSE data analysis, eigen values and eigen functions used for the fitting, and the effect of polydispersity on the bound layer thickness. The Supporting Information is available free of charge on the ACS Publications website at DOI: 10.1021/acsmacrolett.5b00368.

AUTHOR INFORMATION

Corresponding Author
*E-mail: tadanori.koga@stonybrook.edu.
Notes
The authors declare no competing financial interest.

ACKNOWLEDGMENTS

REFERENCES

(1) Balazs, A. C.; Emrick, T.; Russell, T. P. Science 2006, 314, 1107−1110.
(2) Ebbesen, T. W.; Lezec, H. J.; Hiura, H.; Bennett, J. W.; Ghaemi, H. F.; Thio, T. Nature 1996, 382, 54−56.
(3) Ajayan, P. M.; Schadler, L. S.; Braum, P. V. Nanocomposite Science and Technology; Wiley-VCH: Weinheim, Germany, 2003.
(4) Oberdisse, J. Soft Matter 2006, 2, 29−36.
(5) Blum, F. D.; Xu, G.; Liang, M.; Wade, C. G. Macromolecules 1996, 29, 8740−8745.
(6) Lin, W. Y.; Blum, F. D. Macromolecules 1998, 31, 4135−4142.
(7) Litvinov, V. M.; Steeman, P. A. M. Macromolecules 1999, 32, 8476−8490.
(8) Litvinov, V. M.; Orza, R. A.; Kluppel, M.; van Duin, M.; Magusin, P. C. M. M. Macromolecules 2011, 44, 4887−4900.
(9) Harton, S. E.; Kumar, S. K.; Yang, H. C.; Koga, T.; Hicks, K.; Lee, E.; Mijovic, J.; Liu, M.; Vallery, R. S.; Gidley, D. W. Macromolecules 2010, 43, 3415−3421.
(10) Jouault, N.; Moll, J. F.; Meng, D.; Windsor, K.; Ramcharan, S.; Kearney, C.; Kumar, S. K. ACS Macro Lett. 2013, 2, 371−374.
(11) Villars, D. S. J. Polym. Sci. 1956, 21, 257−271.
(12) Medalia, A. I. J. Colloid Interface Sci. 1970, 32, 115−131.

(13) Blow, C. M. *Polymer* **1973**, *14*, 309−323.

(14) Dannenberg, E. M. *Rubber Chem. Technol.* **1986**, *59*, 512−524.

(15) Kenny, J. C.; McBrierty, V. J.; Rigbi, Z.; Douglass, D. C. *Macromolecules* **1991**, *24*, 436−443.

(16) Karasek, L.; Sumita, M. *J. Mater. Sci.* **1996**, *31*, 281−289.

(17) Heinrich, G.; Vilgis, T. A. *Rubber Chem. Technol.* **1995**, *68*, 26−36.

(18) Stickney, P. B.; Falb, R. D. *Rubber Chem. Technol.* **1964**, *37*, 1299−1340.

(19) Papon, A.; Saalwachter, K.; Schaler, K.; Guy, L.; Lequeux, F.; Montes, H. *Macromolecules* **2011**, *44*, 913−922.

(20) Mujtaba, A.; Keller, M.; Ilisch, S.; Radusch, H. J.; Beiner, M.; Thurn-Albrecht, T.; Saalwachter, K. *ACS Macro Lett.* **2014**, *3*, 481−485.

(21) Ciprari, D.; Jacob, K.; Tannenbaum, R. *Macromolecules* **2006**, *39*, 6565−6573.

(22) Ndoro, T. V. M; Voyiatzis, E.; Ghanbari, A.; Theodorou, D. N.; Bohm, M. C.; Muller-Plathe, F. *Macromolecules* **2011**, *44*, 2316−2327.

(23) Papon, A.; Montes, H.; Hanafi, M.; Lequeux, F. *Phys. Rev. Lett.* **2012**, *108*, 065702.

(24) Hooper, J. B.; Schweizer, K. S. *Macromolecules* **2006**, *39*, 5133−5142.

(25) Krutyeva, M.; Wischnewski, A.; Monkenbusch, M.; Willner, L.; Maiz, J.; Mijangos, C.; Arbe, A.; Colmenero, J.; Radulescu, A.; Holderer, O.; Ohl, M.; Richter, D. *Phys. Rev. Lett.* **2013**, *110*, 110.

(26) Ashkar, R.; Abdul Baki, M.; Tyagi, M.; Faraone, A.; Butler, P.; Krishnamoorti, R. *ACS Macro Lett.* **2014**, *3*, 1262−1265.

(27) Goritz, D.; Raab, H.; Frohlich, J.; Maier, P. G. *Rubber Chem. Technol.* **1999**, *72*, 929−945.

(28) Higgins, J. S.; Benoit, H. C. *Polymers and Neutron Scattering*; Oxford University Press: New York, 1994.

(29) The bound polymer layer is mainly resulted from physical adsorption of polymer chains onto the CB filler surface via surface functionalities, while a small amount of chemical cross-links and/or grafting of rubber chains onto the filler surface exist.[8]

(30) Beaucage, G. *J. Appl. Crystallogr.* **1995**, *28*, 717−728.

(31) Takenaka, M.; Nishitsuji, S.; Amino, N.; Ishikawa, Y.; Yamaguchi, D.; Koizumi, S. *Rubber Chem. Technol.* **2012**, *85*, 157−164.

(32) Koga, T.; Takenaka, M.; Aizawa, K.; Nakamura, M.; Hashimoto, T. *Langmuir* **2005**, *21*, 11409−11413.

(33) Koga, T.; Hashimoto, T.; Takenaka, M.; Aizawa, K.; Amino, N.; Nakamura, M.; Yamaguchi, D.; Koizumi, S. *Macromolecules* **2008**, *41*, 453−464.

(34) Kanaya, T.; Monkenbusch, M.; Watanabe, H.; Nagao, M.; Richter, D. *J. Chem. Phys.* **2005**, *122*, 144905.

(35) Jiang, N.; Shang, J.; Di, X.; Endoh, M. K.; Koga, T. *Macromolecules* **2014**, *47*, 2682−2689.

(36) Karim, A.; Satija, S. K.; Douglas, J. F.; Ankner, J. F.; Fetters, L. J. *Phys. Rev. Lett.* **1994**, *73*, 3407−3410.

(37) Rouse, P. E. *J. Chem. Phys.* **1953**, *21*, 1272−1280.

(38) Zimm, B. H. *J. Chem. Phys.* **1956**, *24*, 269−278.

(39) Farago, B.; Monkenbusch, M.; Richter, D.; Huang, J. S.; Fetters, L. J.; Gast, A. P. *Phys. Rev. Lett.* **1993**, *71*, 1015−1018 (It should be noted that the q dependence of the plateau observed in Figure 2 indicates a change in the ratio between the static (i.e., $S(q)$) and fluctuation (i.e., the second term of the denominator of the right hand side of eq 5) contributions to $I(q,t)/I(q,0)$ at $t \to \infty$.).

(40) Fytas, G.; Anastasiadis, S. H.; Seghrouchni, R.; Vlassopoulos, D.; Li, J. B.; Factor, B. J.; Theobald, W.; Toprakcioglu, C. *Science* **1996**, *274*, 2041−2044.

(41) Yakubov, G. E.; Loppinet, B.; Zhang, H.; Ruhe, J.; Sigel, R.; Fytas, G. *Phys. Rev. Lett.* **2004**, *92*, 115501.

(42) de Gennes, P. G. *C. R. Acad. Sci. Paris Ser. II* **1986**, *302*, 765−768.

(43) de Gennes, P. G. *Scaling Concepts in Polymer Physics*; Cornell University Press: Ithaca, New York, 1979.

(44) Koopal, L. K.; Lyklema, J. *Faraday Discuss. Chem. Soc.* **1975**, *59*, 230−241.

(45) Carasso, M. L.; Rowlands, W. N.; O'Brien, R. W. *J. Colloid Interface Sci.* **1997**, *193*, 200−214.

(46) Kritikos, G.; Terzis, A. F. *Eur. Polym. J.* **2013**, *49*, 613−629.

(47) There are some deviations between the experimental and computed $I(q,t)/I(q,0)$ of the breathing model at $t > 1$ ns. At this moment, it is not clear whether the deviation is physically meaningful. But one possibility of the deviation may be slow dynamics of the inner unswollen region, which is ignored for the present data analysis. Further experiments to extend the time scale up to a few hundred ns at high flux neutron facilities are needed.

(48) Daoulas, K. C.; Harmandaris, V. A.; Mavrantzas, V. G. *Macromolecules* **2005**, *38*, 5780−5795.

(49) It should be noted that the collective dynamics observed corresponds to the average of the tail and loop parts of the swollen bound chains. Further NSE experiments using telechelic polymer chains (i.e., doubly bound chains) and polymer brushes (i.e., single bound chains) on the filler are needed to distinguish the respective dynamics.

(50) Flory, P. J. *Principles of Polymer Chemistry*; Cornell University Press: New York, 1953.

(51) Patton, D.; Knoll, W.; Advincula, R. C. *Macromol. Chem. Phys.* **2011**, *212*, 485−497.

(52) Alexander, S. *J. Phys. (Paris)* **1977**, *38*, 983−987.